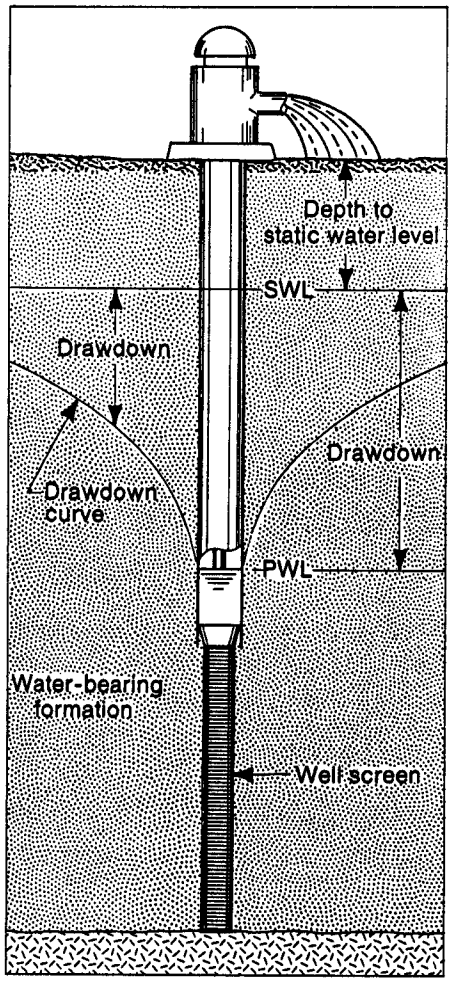

Figure 9.1. Terms relating to well performance.

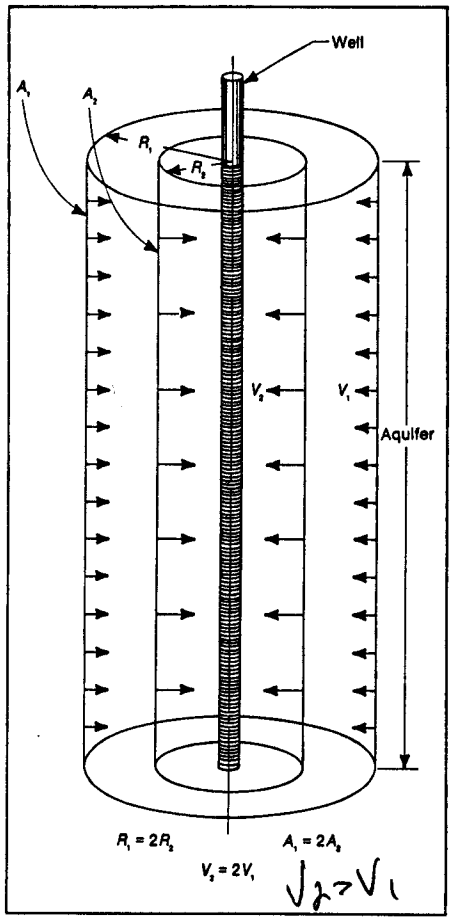

Figure 9.2. As flow converges toward a well, it passes through imaginary cylindrical surfaces that are successively smaller as the well is approached.

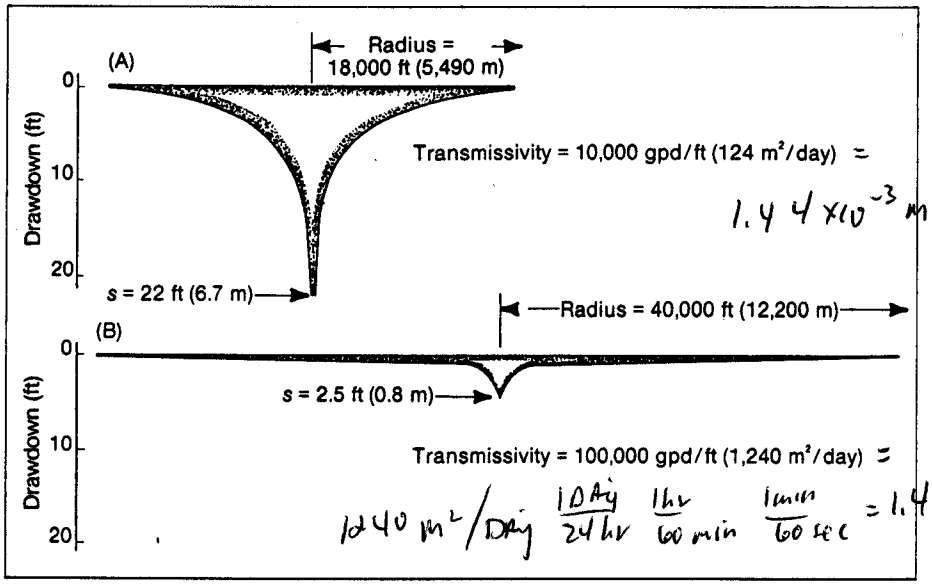

Figure 9.3. Effect of different coefficients of transmissivity on the shape, depth, and extent of the cone of depression. Pumping rate and other factors are constant.

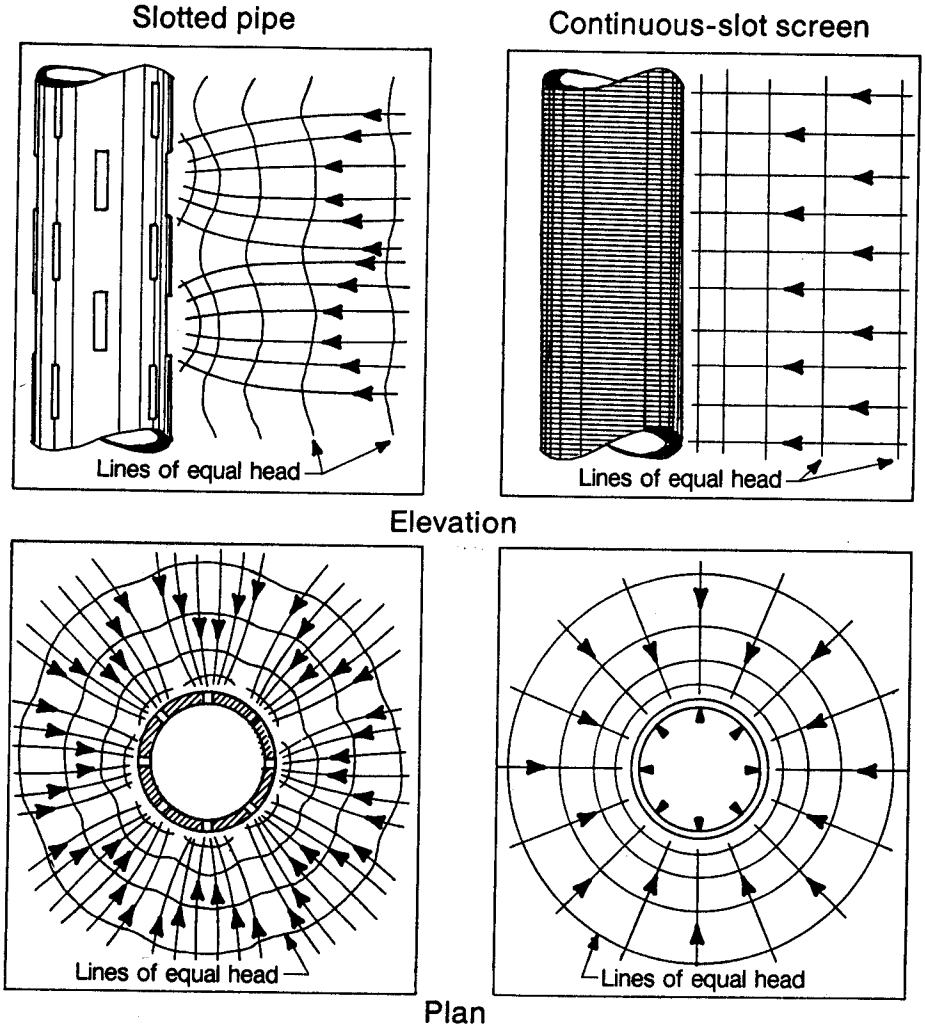

Figure 9.32. Flow nets around screen devices. Water approaches openings along lines indicated by arrows. Flow lines for slotted pipe converge to individual slots; flow lines for continuous-slot well screens are less distorted.

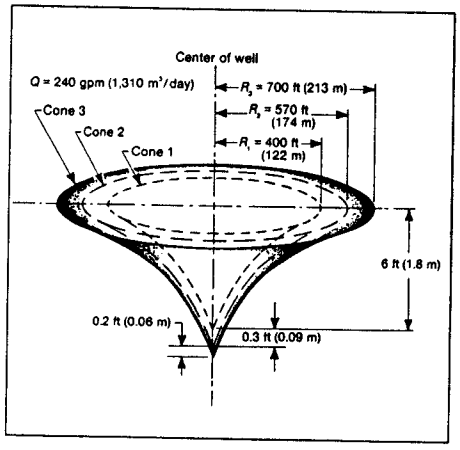

Figure 9.7. Changes in radius and depth of cone of depression after equal intervals of time, at constant pumping rate.

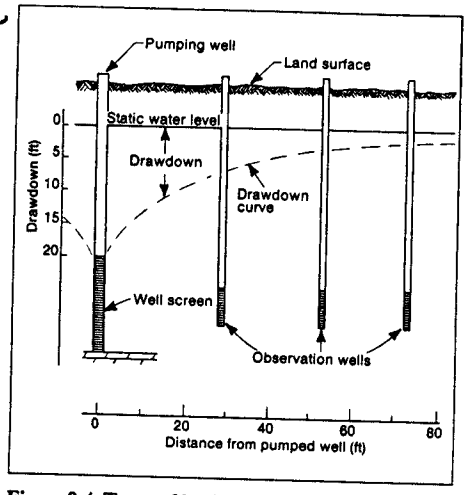

Figure 9.4. Trace of half a cone of depression showing variations in drawdown with distance from a pumped well.

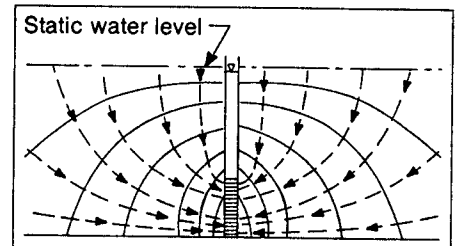

A. Initial stage in pumping an unconfined aquifer. At the instant the pump is turned on, water begins to flow toward the well screen.

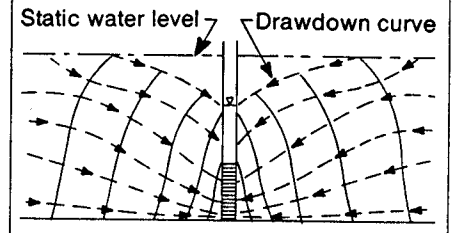

B. Intermediate stage in pumping an unconfined aquifer. Although dewatering of the aquifer materials near the well bore continues, the radial component of flow becomes more pronounced.

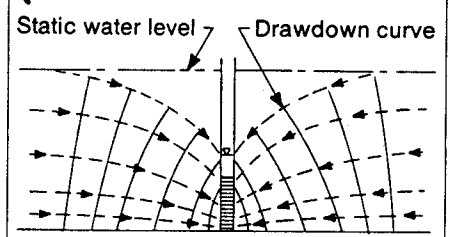

C. Approximate steady state stage in pumping an unconfined aquifer. Profile of cone of depression is established. Nearly all water originates near the outer edge of the area of influence, and a stable, mainly radial flow pattern is established.

Figure 9.6. Development of flow distribution about a discharging well in an unconfined aquifer that is 33% screened. *(Water and Power Resources Service, 1981)*

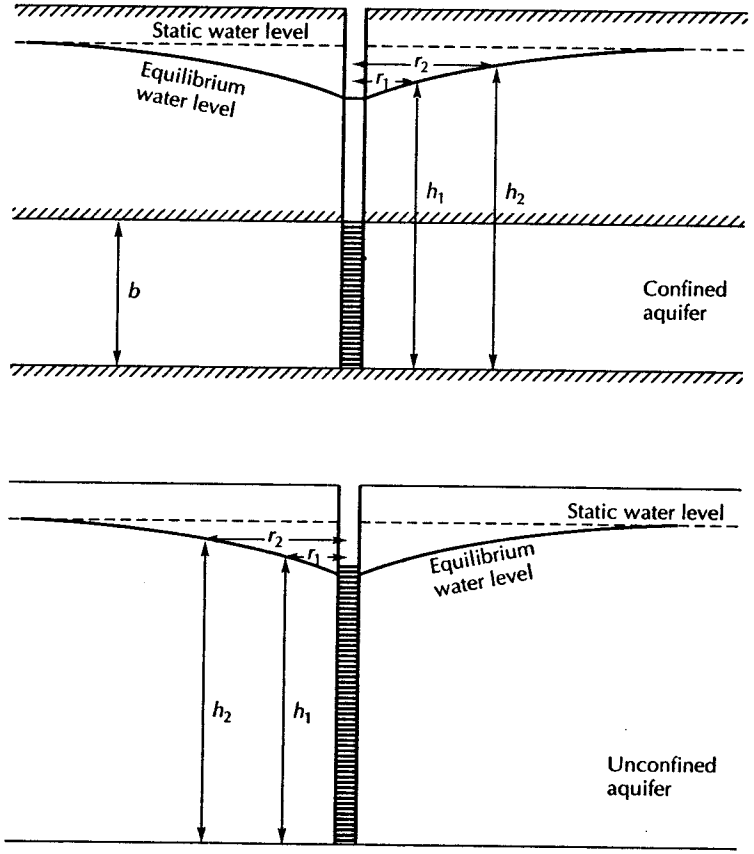

FIGURE 7.5 Equilibrium drawdown: A. confined aquifer; B. unconfined aquifer.

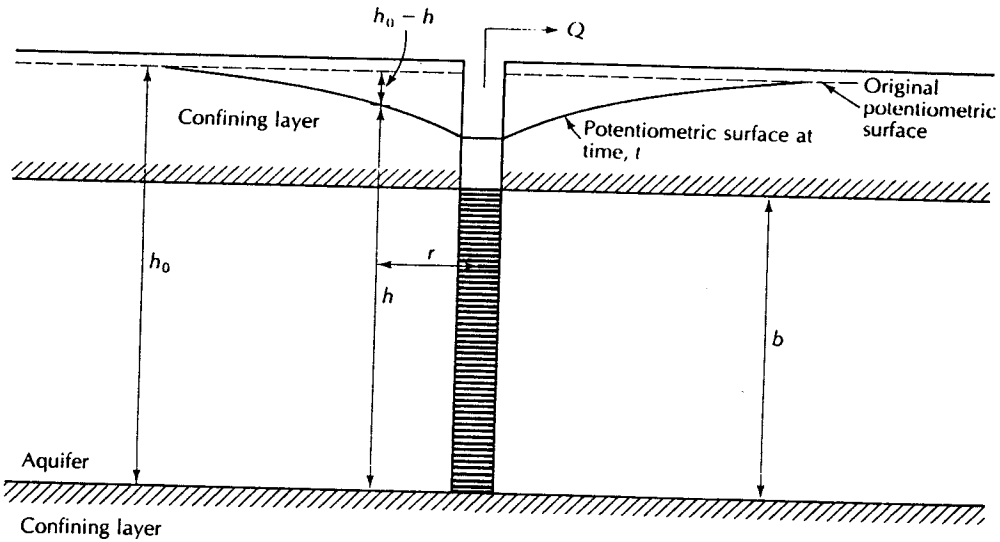

FIGURE 7.2 Fully penetrating well pumping from a confined aquifer.

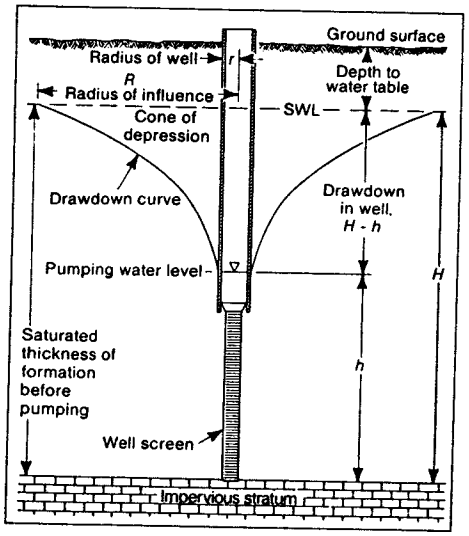

Figure 9.8. Well in an unconfined aquifer showing the meaning of the various terms used in the equilibrium equation.

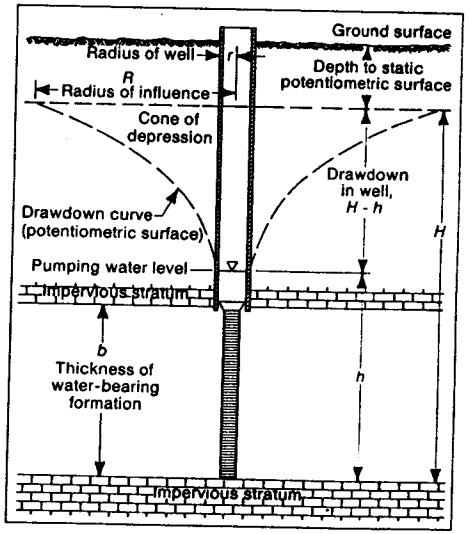

Figure 9.9. Well in a confined aquifer showing the meaning of various terms used in the equilibrium equation.

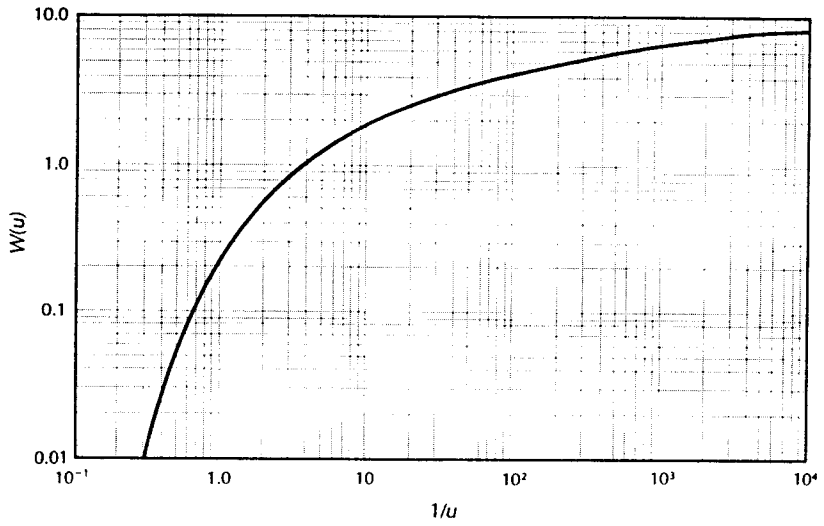

FIGURE 7.6 The nonequilibrium reverse type curve (Theis curve) for a fully confined aquifer.

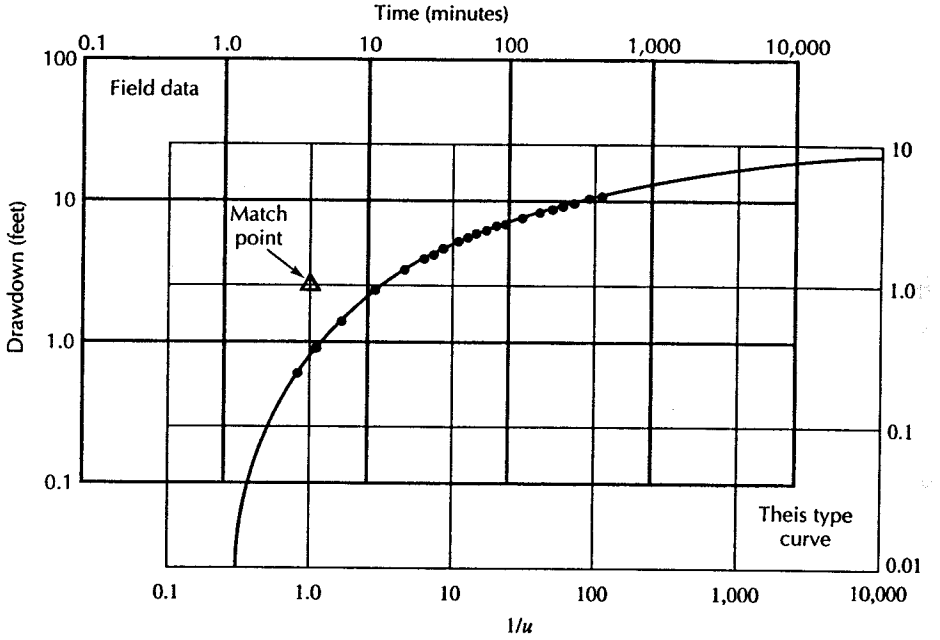

FIGURE 7.8 Match of field-data plot to Theis type curve.

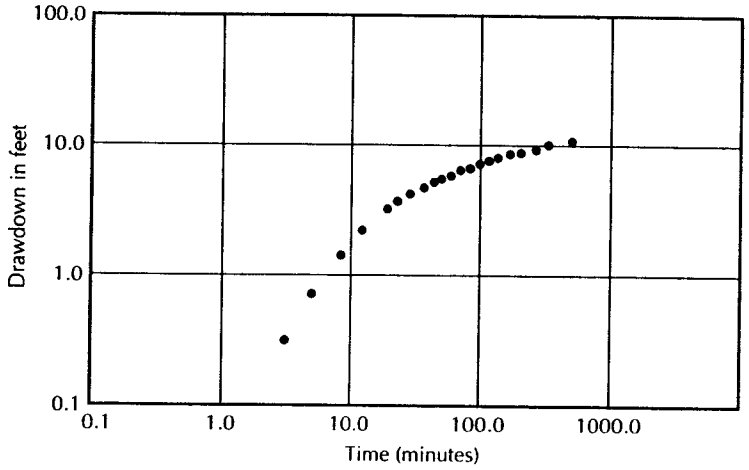

FIGURE 7.7 Field-data plot on logarithmic paper for Theis curve-matching technique.

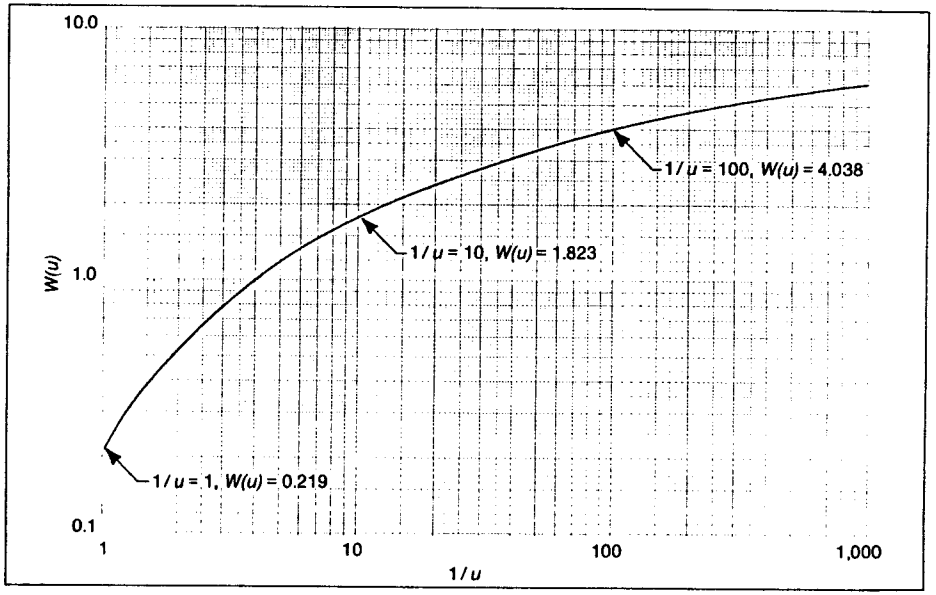

Figure 9.45. Type curve for graphic solution of Theis nonequilibrium equation shows values of *W(u)*, well function of *u*, corresponding to values of 1/*u*. Curve is plotted on logarithmic graph paper.

7.4.3.3 *Nonequilibrium Radial Flow in a Confined Aquifer—Jacob Straight-Line Distance-Drawdown Method*

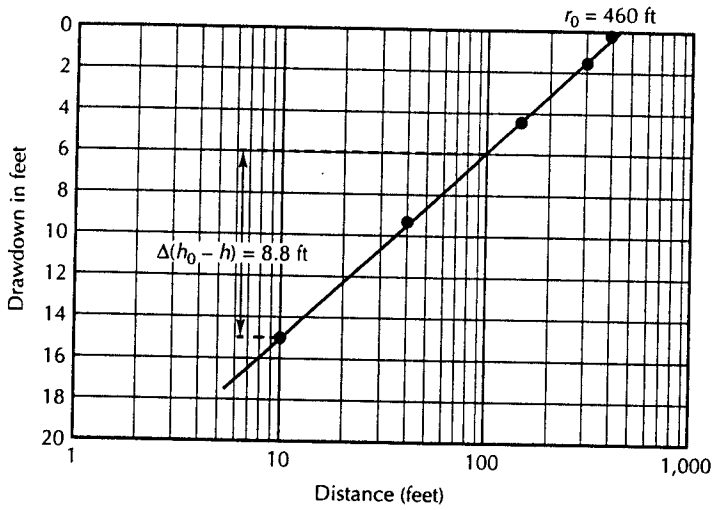

FIGURE 7.10 Variation of the Jacob method of solution of pumping-test data for a fully confined aquifer. Drawdown is plotted as a function of distance to observation well on semilogarithmic paper.

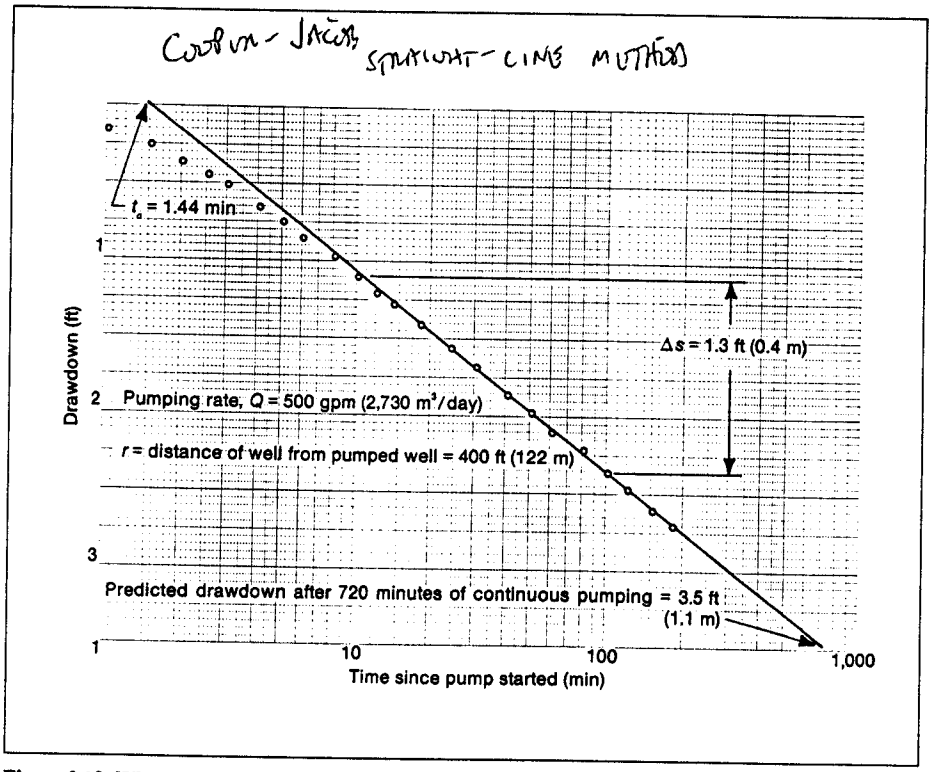

Figure 9.13. When data from Table 9.1 are plotted on semilogarithmic graph paper, most of the plotted points fall on a straight line. The reason for determining Δs and t_0 are explained in the text.

EFFECT OF PARTIAL PENETRATION

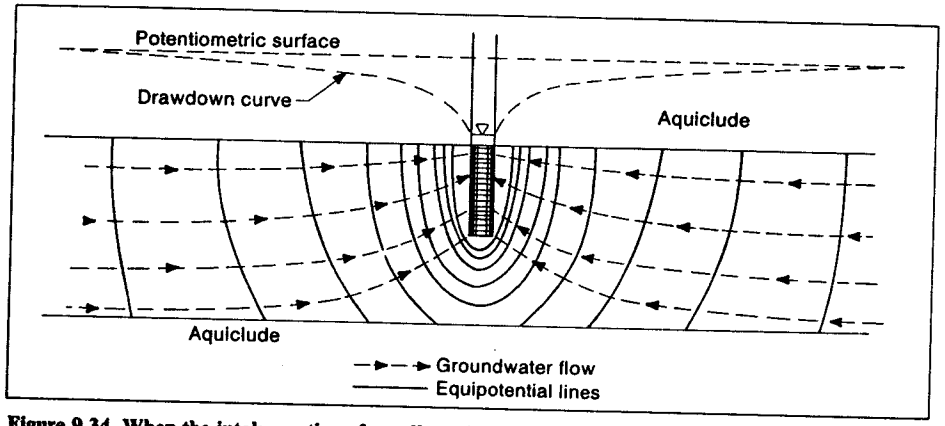

Figure 9.34. When the intake section of a well partially penetrates a confined aquifer, flow lines deviate somewhat from the radial flow pattern associated with a fully penetrating well. *(Water and Power Resources Service, 1981).*

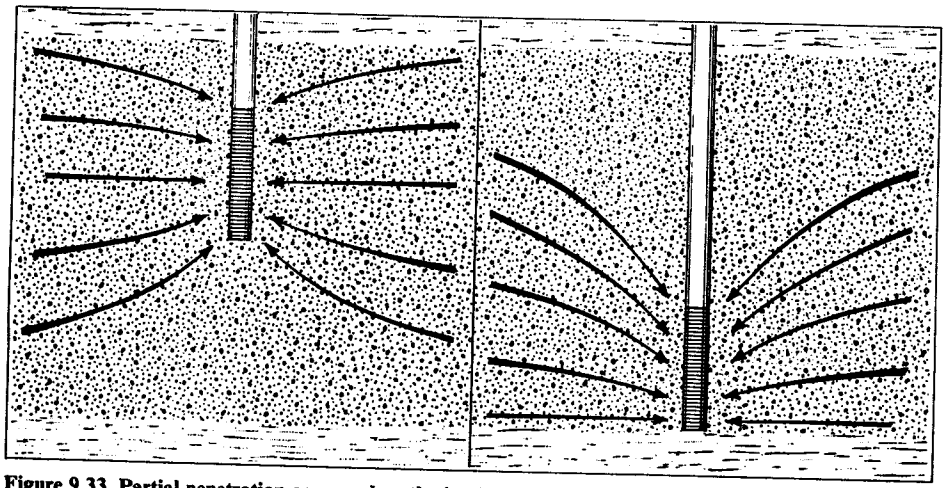

Figure 9.33. Partial penetration occurs when the intake portion of the well is less than the full thickness of the aquifer. This causes distortion of the flow lines and greater head losses.

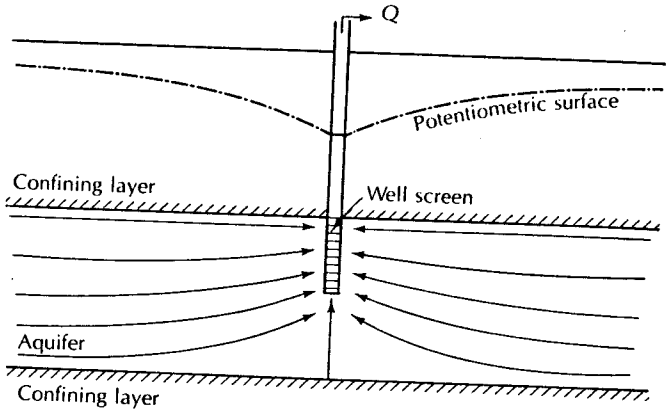

FIGURE 7.17 Flow lines toward a partially penetrating well in a confined aquifer.

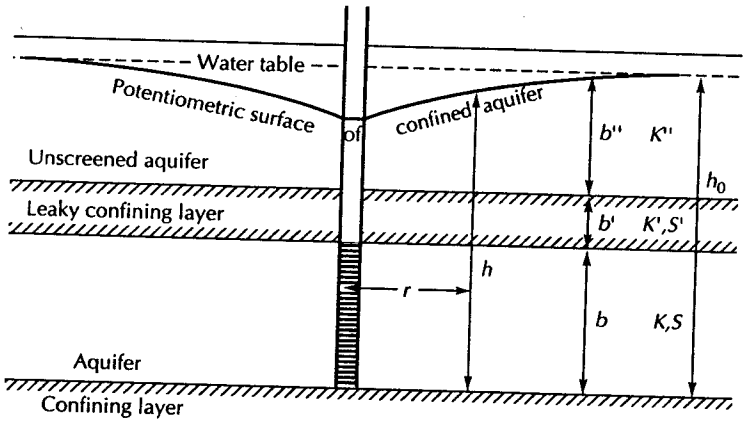

FIGURE 7.3 Fully penetrating well in an aquifer overlain by a semipermeable confining layer.

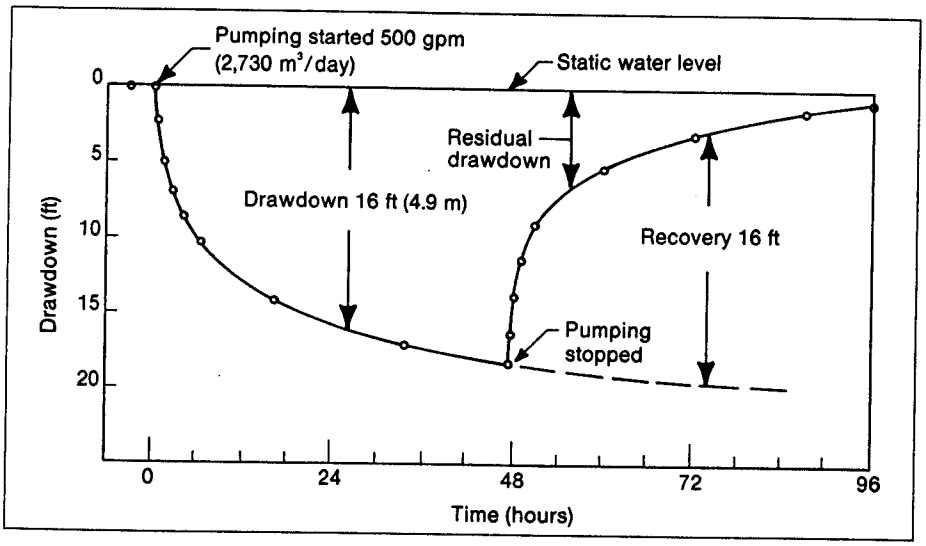

Figure 9.37. Typical drawdown and recovery plots for a well pumped for 48 hours at a constant rate of 500 gpm (2,730 m³/day) followed by a 2-day period for water-level recovery.

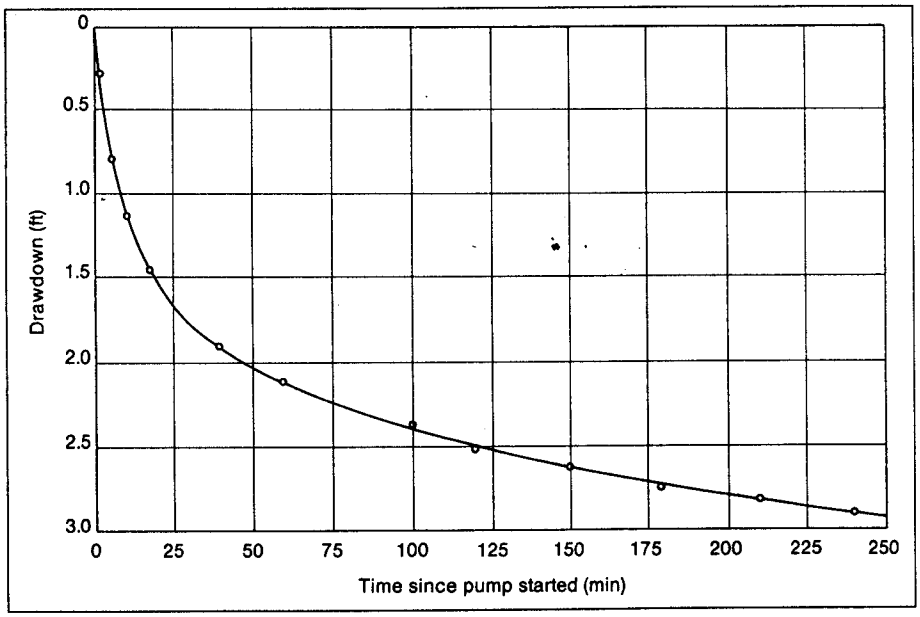

Figure 9.46. Data given in Table 9.1, plotted on ordinary graph paper, show how drawdown varies with duration of pumping. Water level drops rapidly at first, but rate of lowering decreases as pumping continues at 500 gpm (2,730 m³/day). Proper analysis of the test data requires use of the Theis non-equilibrium concept.

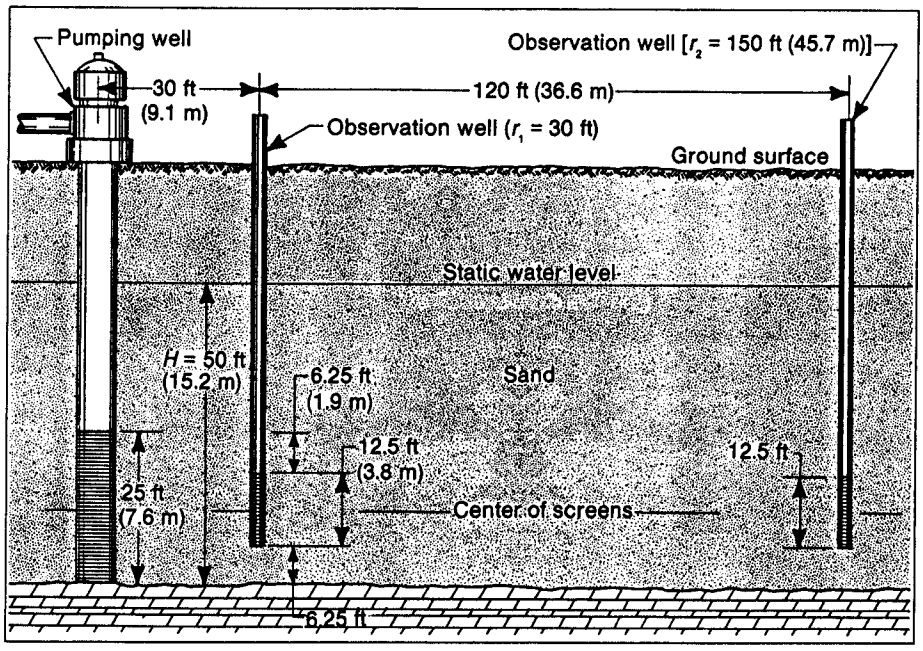

Figure 9.10. Typical arrangement of a pumped well and observation wells for obtaining field data required to calculate hydraulic conductivity from well-discharge equations. Observation wells can be placed farther away from a production well in confined conditions and still provide reliable data.

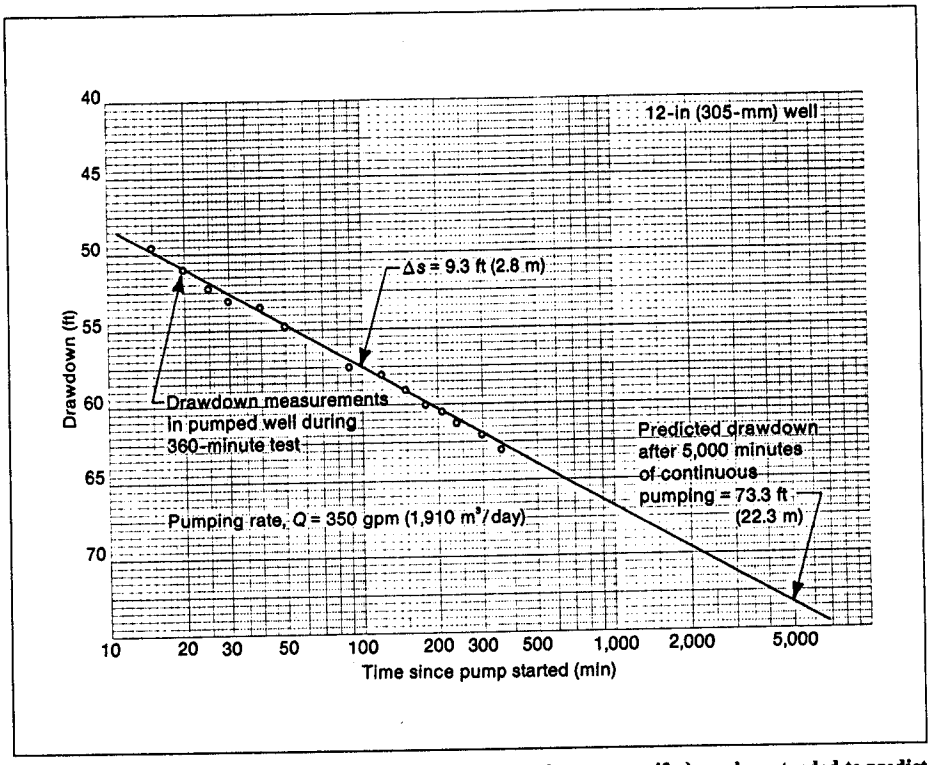

Figure 9.14. Time-drawdown graph for a pumped well (no recharge to aquifer) can be extended to predict drawdown for a period of continuous pumping longer than the test itself.

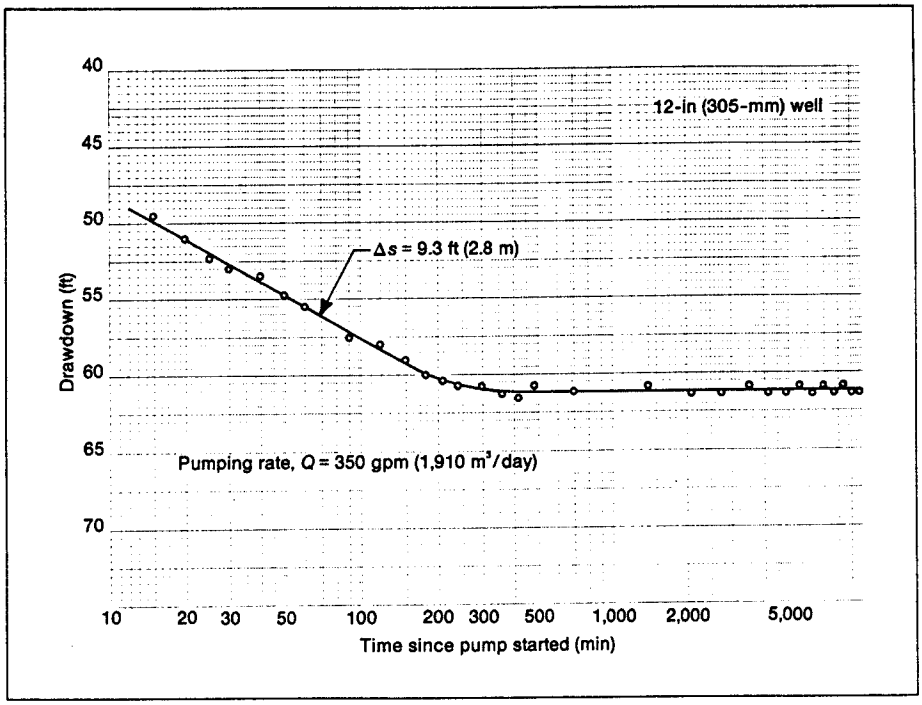

Figure 9.15. When recharge to the aquifer occurs within the zone of influence of the well, the slope of the time-drawdown curve becomes flatter. The horizontal leg indicates that recharge equals well discharge after 240 minutes of pumping.

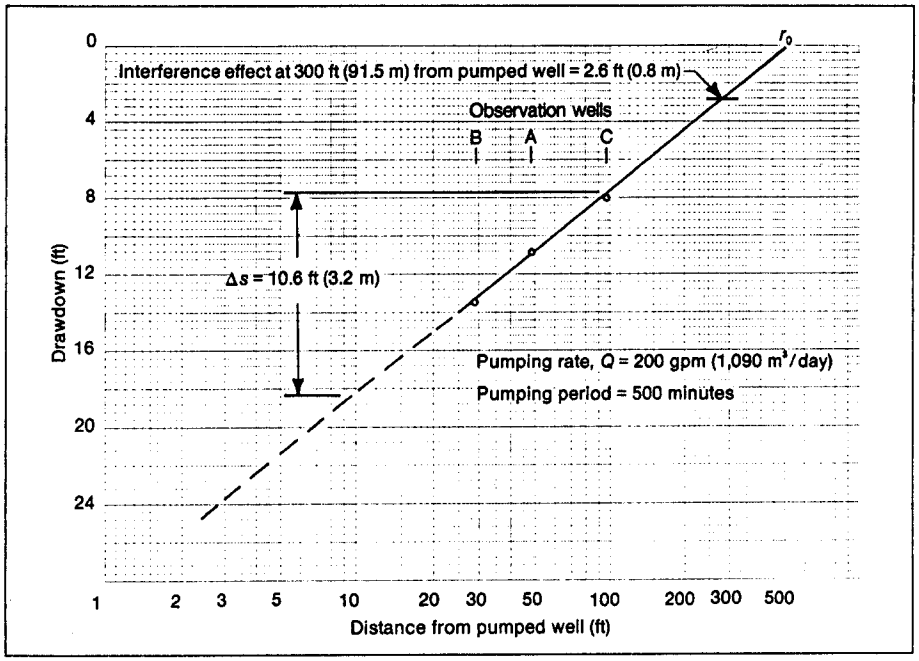

Figure 9.24. Trace of the cone of depression plotted on semilogarithmic graph paper becomes a straight line. Drawdown in each observation well was measured 500 minutes after start of the pumping test.

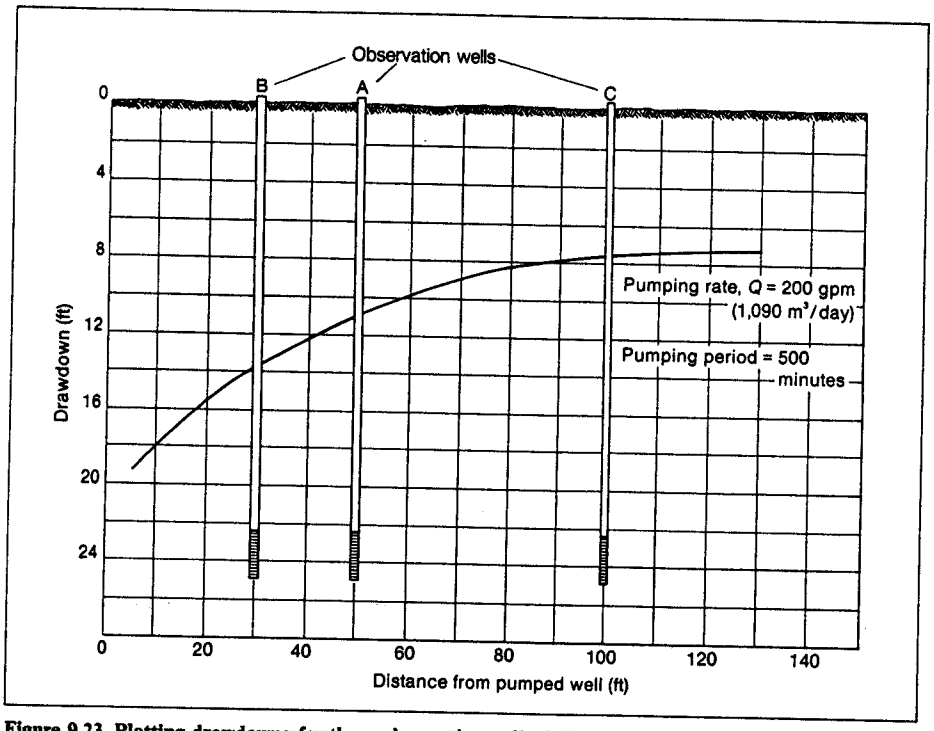

Figure 9.23. Plotting drawdowns for three observation wells defines part of the cone of depression.

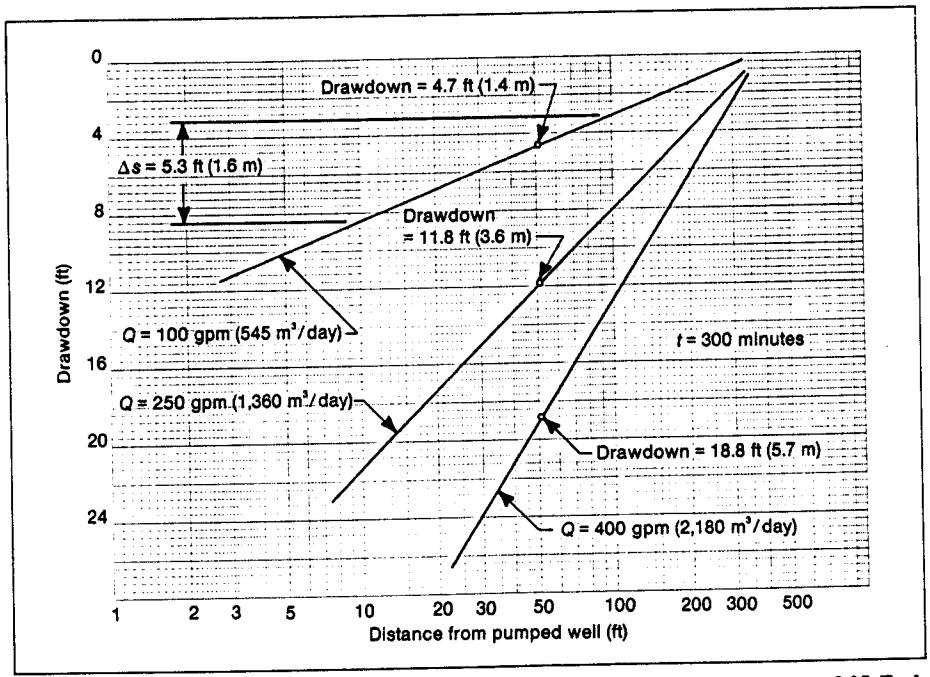

Figure 9.27. Distance-drawdown diagram for various rates of pumping, using data from Figure 9.25. Each plot represents conditions after 300 minutes of pumping at the rate indicated.

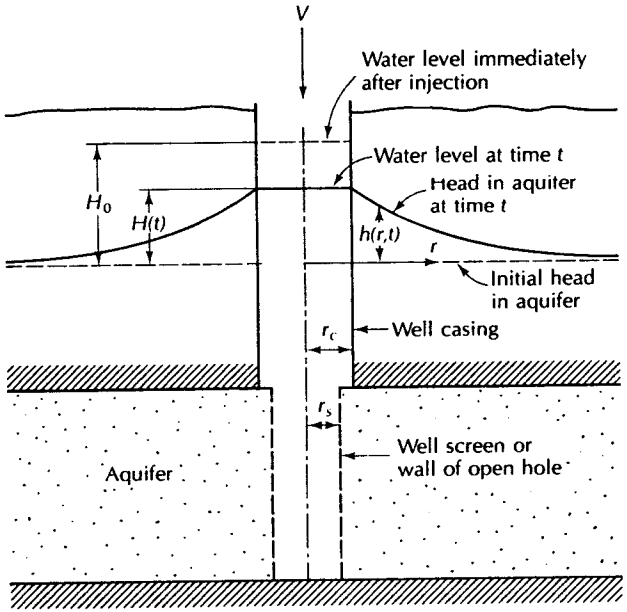

FIGURE 7.18 Well into which a volume, *V*, of water is suddenly injected for a slug test of a confined aquifer. Source: H. H. Cooper, Jr., J. D. Bredehoeft, & I. S. Papadopulos, *Water Resources Research* 3 (1967): 263–9.

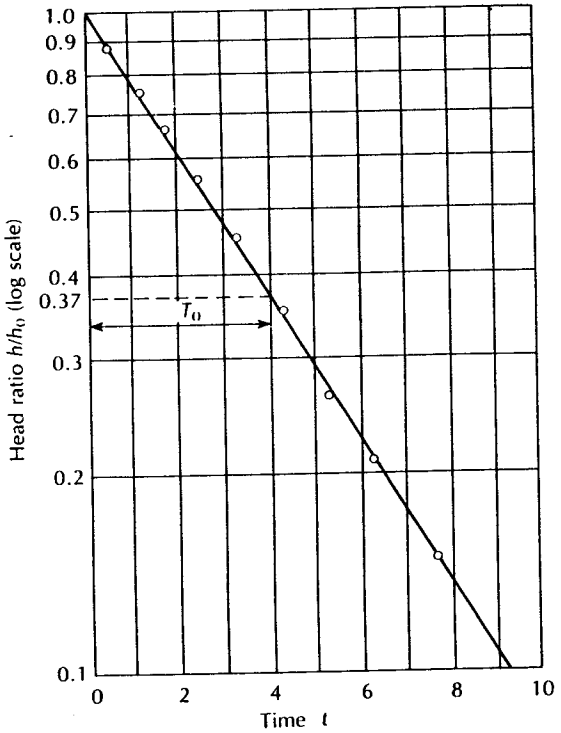

FIGURE 7.22 Plot of head ratio versus time used for Hvorslev method.

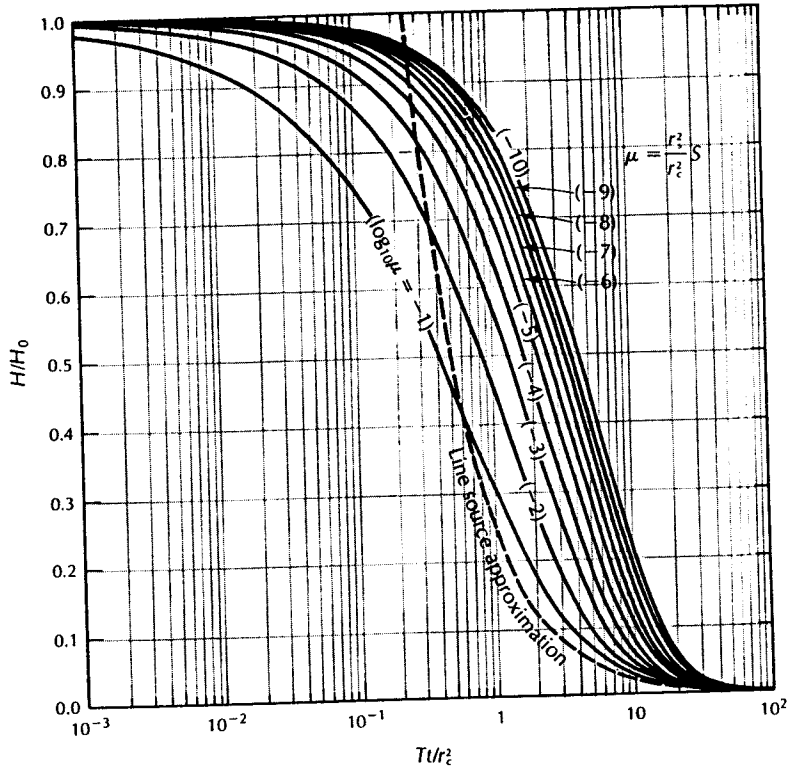

FIGURE 7.19 Type curves for slug test in a well of finite diameter. Source: S. S. Papadopulos, J. D. Bredehoeft, and H. H. Cooper, Jr., *Water Resources Research* 9 (1973): 1087–89.

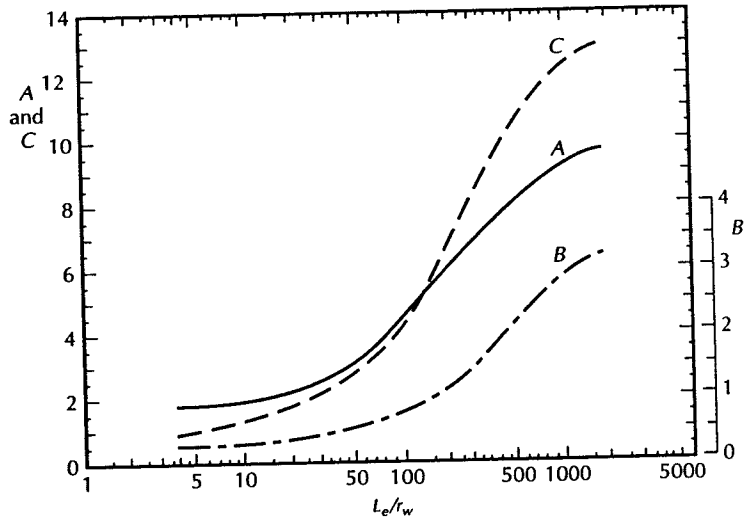

FIGURE 7.25 Dimensionless parameters *A*, *B*, and *C* plotted as a function of L_e/r_w. These parameters are used in the determination of $\ln(R_e/R)$ in Equations 7–87 and 7–88. Source: Herman Bouwer, *Ground Water* 27 (1989): 304–309. Used with permission. © 1989, Ground Water Publishing Company.

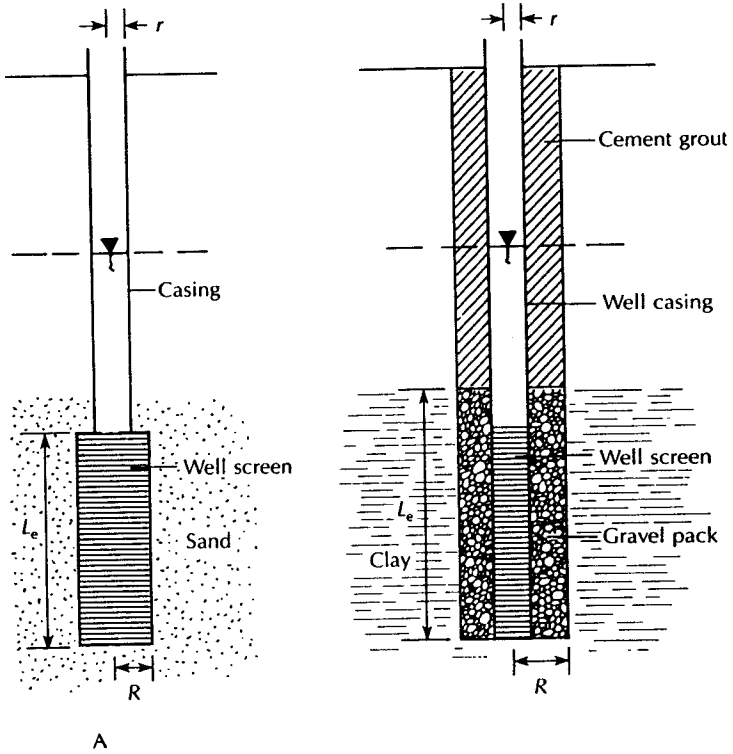

FIGURE 7.21 Piezometer geometry for Hvorslev method. Note that for a piezometer installed in a low-permeability unit the value R is the radius of the highest permeable zone that includes the gravel pack zone and L is the length of the gravel pack zone.

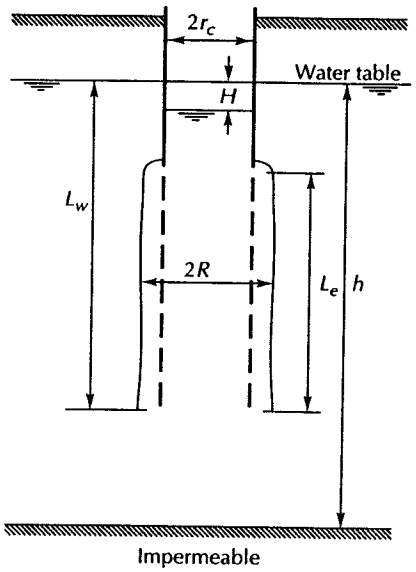

FIGURE 7.24 Geometry and symbols for a slug test on a partially penetrating screened well in an unconfined aquifer with a gravel pack around the screen. Source: Herman Bouwer, *Ground Water* 27 (1989): 304–309. Used with permission. © 1989, Ground Water Publishing Company.

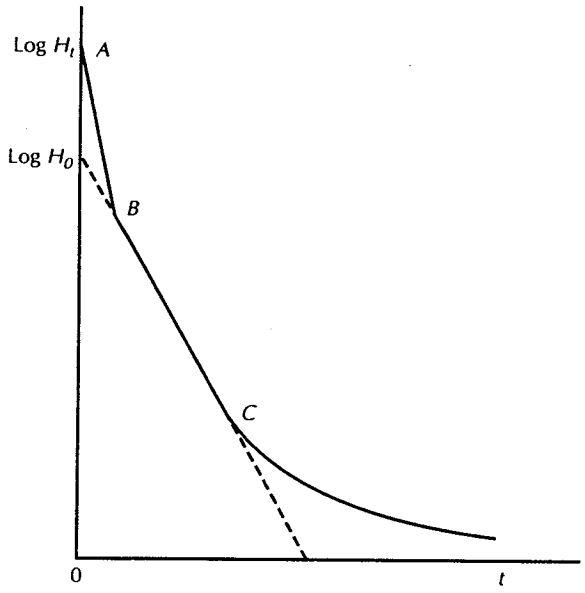

FIGURE 7.27 Head in a borehole as a function of time where two straight-line segments formed during the early part of the test but eventually deviate from the straight line. Sou Herman Bouwer, *Ground Water* 27 (1989): 304–309. Used with permission. © 19 Ground Water Publishing Company.